

## GAMMA-RAY BURST 980329 AND ITS X-RAY AFTERGLOW

J.J.M. in 't Zand<sup>1,2</sup>, L. Amati<sup>3,4</sup>, L.A. Antonelli<sup>5,6</sup>, R.C. Butler<sup>7</sup>, A.J. Castro-Tirado<sup>8,9</sup>,  
A. Coletta<sup>10</sup>, E. Costa<sup>3</sup>, M. Feroci<sup>3</sup>, F. Frontera<sup>11,12</sup>, J. Heise<sup>1</sup>, S. Molendi<sup>13</sup>, L. Nicastro<sup>14</sup>,  
A. Owens<sup>15</sup>, E. Palazzi<sup>11</sup>, E. Pian<sup>11</sup>, L. Piro<sup>3</sup>, G. Pizzichini<sup>11</sup>, M.J.S. Smith<sup>1,10</sup>,  
M. Tavani<sup>13,16</sup>

### ABSTRACT

GRB 980329 is the brightest gamma-ray burst detected so far with the Wide Field Cameras aboard BeppoSAX, both in gamma-rays and X-rays. With

---

<sup>1</sup>Space Research Organization Netherlands, Sorbonnelaan 2, 3584 CA Utrecht, the Netherlands

<sup>2</sup>email jeanz@sron.nl

<sup>3</sup>Istituto di Astrofisica Spaziale (CNR), 00133 Rome, Italy

<sup>4</sup>Istituto Astronomico, Università Degli Studio "La Sapienza", Via Lancisi 29, 00100 Roma, Italy

<sup>5</sup>Osservatorio Astronomico di Roma, Via Frascati 33, 00040 Monteporzio Catone, Italy

<sup>6</sup>BeppoSAX Science Data Center, Via Corcolle 19, 00131 Rome, Italy

<sup>7</sup>Agenzia Spaziale Italiana, Viale Regina Margherita, 00162 Roma, Italy

<sup>8</sup>Laboratorio de Astrofísica Espacial y Física Fundamental (INTA), P.O. Box 50727, 28080 Madrid, Spain

<sup>9</sup>Instituto de Astrofísica de Andalucía (CSIC), P.O. Box 18080, 18080 Granada, Spain

<sup>10</sup>BeppoSAX Scientific Operation Center, Via Corcolle 19, 00131 Rome, Italy

<sup>11</sup>Istituto di Tecnologie e Studio delle Radiazioni Extraterrestri (CNR), Via Gobetti 101, 40129 Bologna, Italy

<sup>12</sup>Dipartimento Fisica, Università di Ferrara, Via Paradiso 12, 44100 Ferrara, Italy

<sup>13</sup>Istituto Fisica Cosmica e Tecnologie Relative (CNR), Via Bassini 15, 20133 Milan, Italy

<sup>14</sup>Istituto Fisica Cosmica e Applicazioni all'Informatica (CNR), Via Ugo La Malfa 153, 90146 Palermo, Italy

<sup>15</sup>Astrophysics Division, Space Science Department of ESA, ESTEC, P.O. Box 299, 2200 AG Noordwijk, the Netherlands

<sup>16</sup>Columbia Astrophysics Laboratory, Columbia University, New York, NY 10027, U.S.A.

respect to its fluence ( $2.6 \times 10^{-5}$  erg s<sup>-1</sup>cm<sup>-2</sup> in 50 to 300 keV) it would be in the top 4% of gamma-ray bursts in the 4B catalog (Meegan et al. 1998). The time-averaged burst spectrum from 2 to 20 and 70 to 650 keV can be well described by the empirical model of Band et al. (1993). The resulting photon index above the break energy is exceptionally hard at  $-1.32 \pm 0.03$ . An X-ray afterglow was detected with the narrow-field instruments aboard BeppoSAX 7 h after the event within the error box as determined with the Wide Field Cameras. Its peak flux is  $(1.4 \pm 0.2) \times 10^{-12}$  erg s<sup>-1</sup>cm<sup>-2</sup> (2 to 10 keV). The afterglow decayed according to a power law function with an index of  $-1.35 \pm 0.03$ . GRB 980329 is characterized by being bright and hard, and lacking strong spectral evolution.

*Subject headings:* Gamma-rays: bursts – X-rays: general

## 1. Introduction

After its launch in April 1996, the Wide Field Camera (WFC) instrument on board the BeppoSAX satellite opened an important window to the understanding of the gamma-ray burst (GRB) phenomenon. Through quick (within a few hours) and accurate (within a few arcminutes) localizations it has enabled for the first time quick (within less than a day) and sensitive multi-wavelength follow-up observations of a number of GRBs. This has resulted in first time detections of afterglows in a broad wavelength range. Two optical counterparts have revealed redshifts which, if interpreted as due to the expansion of the universe, place them at cosmological distances (Metzger et al. 1997, Kulkarni et al. 1998).

Up to July 22, 1998, WFC provided arcminute positions for 14 GRBs. The All-Sky Monitor (ASM) on board the Rossi X-ray Timing Explorer (e.g., Levine et al. 1996) provided such quick positions in 3 additional cases. Of these 17 bursts, 13 were followed up within a day in X-rays with sensitivities down to roughly  $10^{-13}$  erg s<sup>-1</sup>cm<sup>-2</sup> in 2 to 10 keV. All of these resulted in good candidates for X-ray afterglows. Most of the afterglows decayed in a manner consistent with power law functions with indices ranging from  $-1.1$  for GRB 970508 (Piro et al. 1998) to  $-1.57$  for GRB 970402 (Nicastro et al. 1998). In two cases (GRB 970508, Piro et al. 1998, and GRB 970828, Yoshida et al. 1998) extra variability on top of the power law decay was observed.

We here discuss the tenth GRB localized with BeppoSAX-WFC, GRB 980329. The quick distribution of the position (Frontera et al. 1998a, In 't Zand et al. 1998) resulted in the detection of a variable radio counterpart that peaked about 3 days after the burst

(Taylor et al. 1998). Observations of the position of this radio source revealed a candidate host galaxy (Djorgovski et al. 1998) and fading coincident counterparts in the I band (Klose et al. 1998), K band (Larkin et al. 1998, Metzger et al. 1998) and R band (Palazzi et al. 1998). The R-band counterpart decayed in a manner consistent with a power law decay with an index of  $-1.3$ . The optical magnitudes suggest a red spectrum which Palazzi et al. (1998) suggest may be due to substantial absorption in a starburst galaxy.

GRB 980329 is an exceptional case within the set of WFC-detected bursts: it is the brightest at gamma-rays as well as X-rays. Thus, GRB 980329 provides an opportunity to probe previously unexplored parts of the parameter space. We here present gamma-ray and X-ray measurements, both of the burst event and the afterglow of GRB 980329.

## 2. Observations

All GRB and X-ray afterglow measurements presented here were obtained with three sets of instruments on board BeppoSAX (Boella et al. 1997a). The Gamma-Ray Burst Monitor (GRBM, Feroci et al. 1997, Costa et al. 1998) consists of the 4 lateral shields of the Phoswich Detector System (PDS, Frontera et al. 1997) and has a bandpass of 40 to 700 keV. The normal directions of two shields are each co-aligned with the viewing direction of a WFC unit. Therefore, a WFC-detected GRB has a near to optimum GRBM collecting area. The GRBM has 4 basic data products per shield for a GRB: a time history of the 40 to 700 keV intensity with a variable time resolution of up to 0.48 ms, 1 s time histories in 40 to 700 and  $>100$  keV, and a 256 channel spectrum accumulated each 128 s (independently phased from GRB trigger times; 240 of these channels contain scientific data up to 650 keV).

The WFC instrument (Jager et al. 1997) consists of two coded aperture cameras each with a field of view of  $40^\circ$  by  $40^\circ$  full-width to zero response and an angular resolution of about  $5'$ . The bandpass is 2 to 26 keV.

The narrow field instruments (NFI) include 2 imaging instruments that combined are sensitive to 0.1-10 keV photons: the low-energy and the medium-energy concentrator spectrometer (LECS and MECS respectively, see Parmar et al. 1997 and Boella et al. 1997b respectively). They both have circular fields of view with diameters of  $37'$  and  $56'$ . The other 2, non-imaging, NFI are the PDS (13 to 300 keV), and the high-pressure gas scintillation proportional counter (4 to 120 keV, Manzo et al. 1997).

GRB 980329 triggered the GRBM on March 29.15587, 1998 UT. The peak intensity is  $6.6 \times 10^3$  c s $^{-1}$  in 40 to 700 keV. Simultaneously, the burst was detected in WFC unit

number 2 at an off-axis angle of  $19^\circ$ . The peak intensity was about 6 Crab units in 2 to 26 keV. This is the brightest burst seen with both GRBM and WFC. Nevertheless, the statistical quality of the WFC data is moderate because of the relatively large off-axis angle. The X-ray counterpart to GRB 980329 was localized with the WFC with an error circle radius of  $3'$  (Frontera et al. 1998a). The burst also triggered BATSE on board CGRO (trigger number 6665, Briggs et al. 1998) and was detected above 1 MeV with the COMPTEL instrument on CGRO (Connors et al. 1998).

GRB 980329 was declared a target of opportunity for the NFI and a follow-up observation was started on March 29.4499 UT, 7 h after the burst. The afterglow, 1SAX J0702.6+3850, was quickly identified in the LECS and MECS (In 't Zand et al. 1998). The time span of the observation is 41.5 h. An interruption occurred between 21.2 and 27.5 h after the start. The total net exposure times are 25 ks for the LECS and 64 ks for the MECS.

### 3. Analysis

#### 3.1. The burst event

The most intense part of the burst has similar durations in X-rays and gamma rays (see figure 1). The full-width at half-maximum duration of the burst is, within 0.5 s, equal to 8.6 s from 2 to 700 keV. The average burst duration versus photon energy relation as defined by Fenimore et al. (1995) for bright bursts predicts a time scale at 10 keV that is  $2\frac{1}{2}$  times larger than that at 100 keV. There is a soft tail in the WFC data not easily discernible in figure 1 but showing up in binned imaging data up until 90 s after the trigger (see figure 3). Beyond 40 keV the burst shows a moderate spectral evolution with a softening trend. The photon index as derived from a power law fit to the two-channel 1 s GRBM data (figure 1c) varies between  $-1.19 \pm 0.06$  and  $-1.96 \pm 0.26$ . A Fourier power spectrum of the high time resolution data of the GRBM shows no features between 3 Hz and 64 Hz.

The 256-channel GRBM data of GRB 980329 permits a sensitive spectral analysis. A 128 s accumulation interval ends 54 s after the burst trigger and covers most of the burst (see figure 1). We have analyzed this spectrum above 70 keV simultaneously with the 2 to 20 keV spectrum measured with WFC from 0 to 54 s (below 70 keV the response matrix of the GRBM is not sufficiently well known, the same applies to the WFC matrix above 20 keV). We employed the GRB spectral model defined by Band et al. (1993) as:

$$N(E) = \begin{cases} AE^\alpha \exp(-E/E_0), & \text{for } E \leq (\alpha - \beta)E_0, \\ BE^\beta, & \text{for } E \geq (\alpha - \beta)E_0 \end{cases}$$

phot  $\text{s}^{-1}\text{cm}^{-2}\text{keV}^{-1}$ , where  $E$  is the photon energy and  $A$  and  $B$  are coupled normalization constants. A fit of this model to the data (see figure 2) reveals  $\alpha = -0.6 \pm 0.2$ ,  $\beta = -1.32 \pm 0.03$  and  $E_0 = 134 \pm 110$  keV ( $\chi_r^2 = 1.07$  for 140 d.o.f.). A broken power law function fits the data just as well (with comparable power law indices). Since  $\beta$  is larger than -2, even in the time-resolved data (see figure 1c), the peak of the  $\nu F_\nu$  spectrum is beyond the high energy boundary of our data set. A single power law model with absorption due to cold matter of cosmic abundances describes the data worse, with  $\chi_r^2 = 1.35$  (141 d.o.f.). The chance probability that  $\chi_r^2$  is at least that high is  $2 \times 10^{-3}$ . Although the WFC and GRBM instruments have not yet been cross calibrated, we anticipate no large relative systematic errors between WFC and GRBM. WFC could be calibrated for this particular observation with a standard calibration source (i.e., the Crab source) in the same field of view. Furthermore, GRBM was calibrated against the Crab source and cross calibrated against BATSE for a number of bursts.

Given the model spectrum, the fluence is  $(7 \pm 1) \times 10^{-7}$  erg  $\text{cm}^{-2}$  in 2 to 10 keV and  $(5.5 \pm 0.5) \times 10^{-5}$  erg  $\text{cm}^{-2}$  in 40 to 700 keV. The former fluence constitutes 1% of the expected 2–700 keV fluence. The 50–300 keV fluence of  $(2.6 \pm 0.3) \times 10^{-5}$  erg  $\text{cm}^{-2}$  would place GRB 980329 in the top 4% of the bursts in the 4B catalog (Meegan et al. 1998).

### 3.2. The X-ray afterglow

The average LECS/MECS spectrum of 1SAX J0702.6+3850 over the first 21 h of the follow-up observation (up until the interruption) could be modeled by a power law function with a photon index of  $\Gamma = -2.4 \pm 0.4$  and a low energy cutoff equivalent to interstellar absorption by a hydrogen column density of  $N_{\text{H}} = (1.0 \pm 0.4) \times 10^{22}$   $\text{cm}^{-2}$  ( $\chi_r^2 = 0.9$  for 28 d.o.f.). The 99% confidence interval for  $N_{\text{H}}$  is  $0.21 - 2.3 \times 10^{22}$   $\text{cm}^{-2}$ . A black body spectrum also fits the data well, the parameters are:  $kT = 1.0 \pm 0.1$  keV,  $N_{\text{H}} < 2.4 \times 10^{22}$   $\text{cm}^{-2}$  (99% confidence level) and  $\chi_r^2 = 1.1$  for 28 d.o.f. An f-test does not rule against either spectral model. The average flux is  $4.0 \times 10^{-13}$  erg  $\text{s}^{-1}\text{cm}^{-2}$  in 2 to 10 keV. The predicted Galactic value for  $N_{\text{H}}$  in the direction of the burst is  $9 \times 10^{20}$   $\text{cm}^{-2}$  (interpolated from the maps by Dickey & Lockman 1990). This is inconsistent with the NFI result on  $N_{\text{H}}$  for the power law model. The value of  $1.9 \times 10^{21}$   $\text{cm}^{-2}$  as implied by the reddening of the optical spectrum (Palazzi et al. 1998) is marginally consistent with this value (the chance probability for two  $N_{\text{H}}$  values being at least as deviant as observed is 0.3%). The data do not allow a sensitive timing analysis of the spectrum. The roughest such analysis reveals that the 3 to 10 keV over 2 to 3 keV hardness ratio changes from  $1.0 \pm 0.2$  to  $0.5 \pm 0.2$  over the two halves of the observation. This is statistically consistent with a constant ratio.

The 13 to 300 keV PDS data of the first 21 h of the follow-up observation show no detection of the afterglow. Assuming the same model spectrum applies as to the LECS and MECS data, the  $3\sigma$  upper limit is  $4 \times 10^{-11}$  erg s $^{-1}$ cm $^{-2}$ . This is two orders of magnitude above the extrapolation of the LECS/MECS spectrum into the PDS bandpass.

A time history of the afterglow was constructed from all MECS data for the 2 to 10 keV bandpass, see figure 3. The time bins were scaled logarithmically in order to optimize the signal-to-noise ratio in each bin. A power law function satisfactorily describes the data, the resulting power law index is  $-1.5 \pm 0.2$  and  $\chi_r^2 = 0.8$  (3 d.o.f.). The trend in the afterglow extends quite close to the WFC measurements of the burst (see figure 3). Therefore, in a next step we included the 2 to 10 keV flux as measured with WFC between 54 and 90 s after the trigger into the model. The best-fit decay index then is  $-1.35 \pm 0.03$  ( $\chi_r^2 = 0.8$  for 4 d.o.f.). It is consistent with the index as determined from the afterglow alone. We conclude that there is evidence that the afterglow emission started during the tail of the burst event. Unfortunately, we cannot substantiate this with spectral measurements because of insufficient statistics.

There is WFC coverage from 24 h before till about 5 h after the burst, with intermissions. No emission was detected from the burst position outside the 90 s interval after the trigger time. The  $3\sigma$  upper limits are  $1 \times 10^{-10}$  erg s $^{-1}$ cm $^{-2}$  for the pre-burst and  $3 \times 10^{-10}$  erg s $^{-1}$ cm $^{-2}$  for the post-burst data (2 to 10 keV)

Greiner et al. (1998) reported a ROSAT observation that started 35 h after the end of the NFI observation and lasted 39 h (Greiner, priv. comm.). No X-ray afterglow was detected. For  $N_H = 1 \times 10^{22}$  cm $^{-2}$ , the ROSAT upper limit in 0.1-2.4 keV for the unabsorbed flux is 3 times the value predicted from an extrapolation of the MECS evolution.

The decay function predicts a 2 to 10 keV fluence (i.e., integrated from 1 s after the trigger onwards) of  $3 \times 10^{-6}$  erg cm $^{-2}$ . In the 2 to 700 keV band the afterglow fluence is one order of magnitude smaller than the fluence of the burst event. The decay index is consistent with that of the R-band counterpart (Palazzi et al. 1998). Also, it is very close to the average of -1.32 over the X-ray afterglows of GRB 970228 (Costa et al. 1997), GRB 970402 (Nicastro et al. 1998), GRB 970508 (Piro et al. 1998), GRB 970828 (Yoshida et al. 1998) and GRB 971214 (Heise et al. 1998).

No flares or dips occur on time scales down to  $10^3$  s. The  $3\sigma$  upper limit on upward fluctuations on a 4000 s time scale is 70% at the start and 240% at the end of the NFI observation. The data is marginally sensitive to detect flux increases like in GRB 970508 (about 200%, Piro et al. 1998) or GRB 970828 (about 100%, Yoshida et al. 1998).

#### 4. Discussion

The spectrum of the burst is exceptionally hard above the break energy during the whole event. Preece et al. (1998) studied the spectra of 126 bright bursts detected with BATSE during 1991 to 1997 above 28 keV, with fluences comparable to or higher than that of GRB 980329. None of these bursts shows a time-averaged  $\beta > -1.51$ . Another study of 22 GRBs detected with GRB sensors on board *Ginga* in the 2 to 400 keV range shows a similar upper boundary of -1.50 (Strohmayr et al. 1998). Our results indicate that in rare cases the radiative conditions applicable to high peak-intensity bursts can favor hard power-law components of the spectrum.

Of all 14 GRBs detected with WFC and GRBM, GRB 980329 is the brightest in both X-rays and gamma-rays. The burst most similar to GRB 980329 is GRB 970111 (Feroci et al. 1998). It has a similar ratio of GRBM to WFC photon count rate during the gamma-ray peak and its gamma-ray peak intensity and fluence are only  $\sim 20\%$  smaller. Furthermore, the durations of both bursts are similar and the gamma-ray time profiles are, by eye, of the same complexity. The difference between both bursts is that the time profile of GRB 970111 shows much more spectral evolution and is softer at high energies as indicated by the average for  $\beta$  of  $-2.13 \pm 0.03$  (Frontera et al. 1998b).

The behavior of the X-ray afterglow of GRB 980329 is quite similar to that of afterglows of other GRBs, both in intensity and decay index (except for GRB 970228 which is brighter). Therefore, in general there does not appear to be strong correlation between burst events and their X-ray afterglow.

GRB afterglow observations generally comply well with the relativistic blast wave model in which relativistic electrons produce synchrotron radiation (e.g., Wijers, Rees & Meszáros 1997; Sari, Piran & Narayan 1998). In this model the spectral evolution is given by  $F(\nu, t) \propto t^\delta \nu^\epsilon$  for a range of frequencies and times which contain no spectral breaks. In each of two states  $\delta$  and  $\epsilon$  are functions of only  $p$ , the power law exponent of the electron Lorentz factor distribution. For the synchrotron cooling stage of the blast wave,  $\epsilon_s = 2\delta/3$ . For the adiabatic cooling stage,  $\epsilon_a = 2\delta/3 - 1/3$ . For  $\delta = -1.35 \pm 0.03$ ,  $\epsilon_s = -0.90 \pm 0.02$  and  $\epsilon_a = -1.23 \pm 0.02$ . The measured value of  $\epsilon = -1.4 \pm 0.4$  complies well to both predictions with a weak preference for adiabatic cooling for which  $p = (-4\delta + 2)/3 = 2.46 \pm 0.04$ .

The brightness of the burst suggests the possibility of a relatively small distance. However, beaming effects may be important and may be related to the lack of strong spectral evolution of the burst and the relative hardness at high energies. A future redshift measurement of the proposed host galaxy (Djorgovski et al. 1998) and a continued monitoring of the radio scintillation (Taylor et al. 1998) may reveal more insight.

We are grateful to the staff of the BeppoSAX Scientific Operation Center, the Mission Planning Team and the Science Data Center for their support in obtaining and processing the data. The BeppoSAX satellite is a joint Italian and Dutch program.

## REFERENCES

- Band, D., et al. 1993, *ApJ*, 413, 281
- Boella, G., et al. 1997a, *A&AS*, 122, 327
- Boella, G., et al. 1997b, *A&AS*, 122, 299
- Briggs, M., Richardson, G., Kippen, R.M., Woods, P.M., 1998, *IAU Circ.* 6856
- Connors, A., Barthelmy, S.D., Butterworth, P., Kippen, R.M., Connaughton, V. 1998, GCN/GRO COMPTEL burst position notices of March 28 and 29, 1998
- Costa, E., et al. 1997, *Nature*, 387, 783
- Costa, E., et al. 1998, *Adv. Sp. Res.*, in press
- Dickey, J.M., Lockman, F.J. 1990, *ARA&A*, 28, 215
- Djorgovski, S.G., et al. 1998, *GCN Circ.* 41
- Fenimore, E.E., in 't Zand, J.J.M., Norris, J.P., Bonnell, J.T., Nemiroff, R.J. 1995, *ApJ*, 448, L101
- Feroci, M., et al. 1997, *Proc. SPIE*, 3114, 186
- Feroci, M., et al. 1998, *A&A*, 332, L29
- Frontera, F., et al. 1997, *A&AS*, 122, 357
- Frontera, F., et al. 1998a, *IAU Circ.* 6853
- Frontera, F., et al. 1998b, in *AIP Conf. Proc.* 428, *Gamma-Ray Bursts*, ed. C.A. Meegan, R.D. Preece, T.M. Koshut (New York: AIP), 446
- Greiner, J., et al. 1998, *GCN Circ.* 59
- Heise, J., et al. 1998, in preparation
- Jager, R., et al. 1997, *A&AS*, 125, 557
- Klose, S., et al. 1998, *GCN Circ.* 43
- Kulkarni, S.R., et al. 1998, *Nature*, 393, 35
- Larkin, J., et al. 1998, *GCN Circ.* 44 and 51
- Levine, A.M., et al. 1996, *ApJ*, 467, L33



- Manzo, G., et al. 1997, *A&AS*, 122, 341
- Meegan, C., et al. 1998, in *AIP Conf. Proc.* 428, *Gamma-Ray Bursts*, ed. C.A. Meegan, R.D. Preece, T.M. Koshut (New York: AIP), 3
- Metzger, M.R., et al. 1997, *Nature*, 387, 879
- Metzger, M.R., et al. 1998, *GCN Circ.* 55
- Nicastro, L., et al. 1998, *A&A*, submitted
- Palazzi, E., et al. 1998, *A&A*, 336, L95
- Parmar, A.N., et al. 1997, *A&AS*, 122, 309
- Piro, L., et al. 1998, *A&A*, 331, L41
- Preece, R.D., et al. 1998, *ApJ*, 496, 849
- Sari, R., Piran, T., Narayan, R. 1998, *ApJ*, 497, L17
- Strohmayer, T.E., Fenimore, E.E., Murakami, T., Yoshida, A. 1998, *ApJ*, 500, 873
- Taylor, G.B., et al. 1998, *ApJ*, 502, L115
- Yoshida, A., et al. 1998, in *AIP Conf. Proc.* 428, *Gamma-Ray Bursts*, ed. C.A. Meegan, R.D. Preece, T.M. Koshut (New York: AIP), 441
- Wijers, R.A.M.J., Rees, M.J., Meszáros, P. 1997, *MNRAS*, 288, L51
- in 't Zand, J.J.M., et al. 1998, *IAU Circ.* 6854

Fig. 1.— Time history of the burst itself as seen with WFC and GRBM, at a time resolution of 1 s (panel a) and 0.25 s resolution (panel b). Panel c refers to the the photon index of a power law function description of the GRBM two-channel data. The horizontal dashed lines refer to the background levels in the raw count rates. These are the averages as determined from the data beyond +90 s.

Fig. 2.— The photon spectrum of GRB 980329 as measured with GRBM between -74 s and +54 s from the trigger time and with WFC between +0 and +54 s. The drawn line refers to the best fit "Band" spectrum (see text).

Fig. 3.— Time history of the X-ray afterglow, based on WFC (first 3 data points) and MECS data (last 5 points). The horizontal bars refer to the times of observation, vertical bars to the  $1\sigma$  errors. The first point is from 15 to 23 s (see figure 1) which is the brightest part of the burst. The calibration of MECS  $\text{c s}^{-1}$  to 2 to 10 keV  $\text{erg s}^{-1}\text{cm}^{-2}$  is based on

the overall LECS/MECS spectrum. The drawn line refers to a power law fit to the data (see text), the dashed line to an extrapolation.

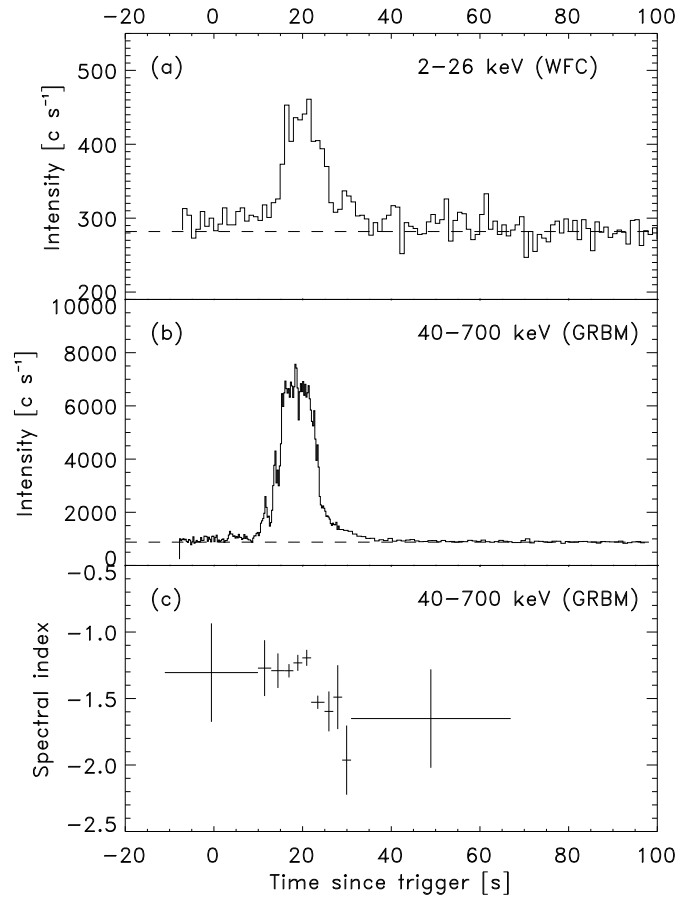


Fig. 1.—

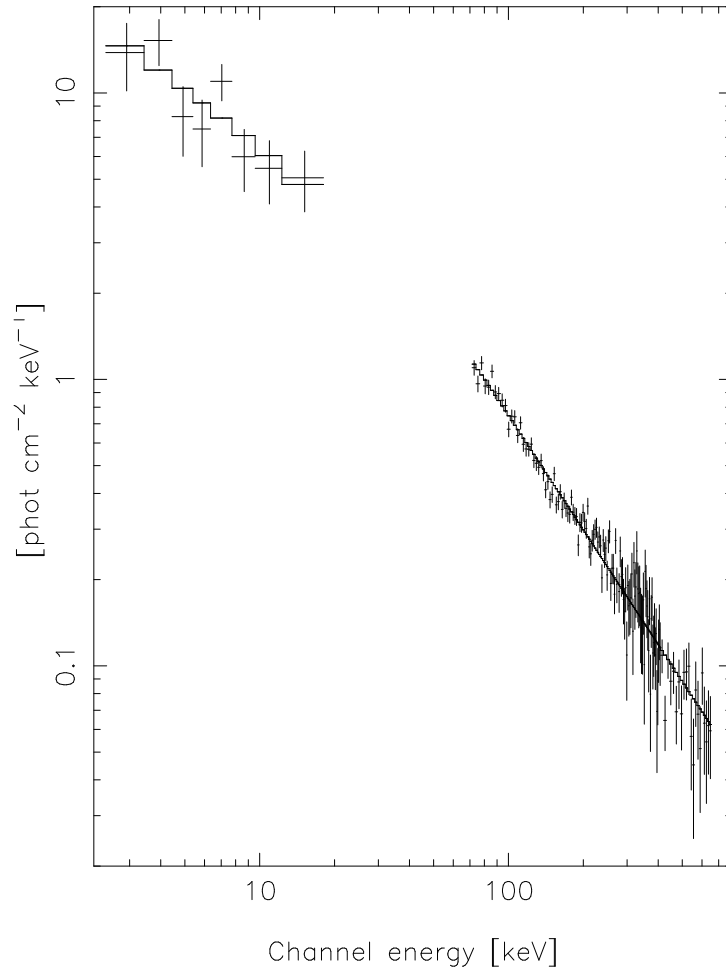


Fig. 2.—

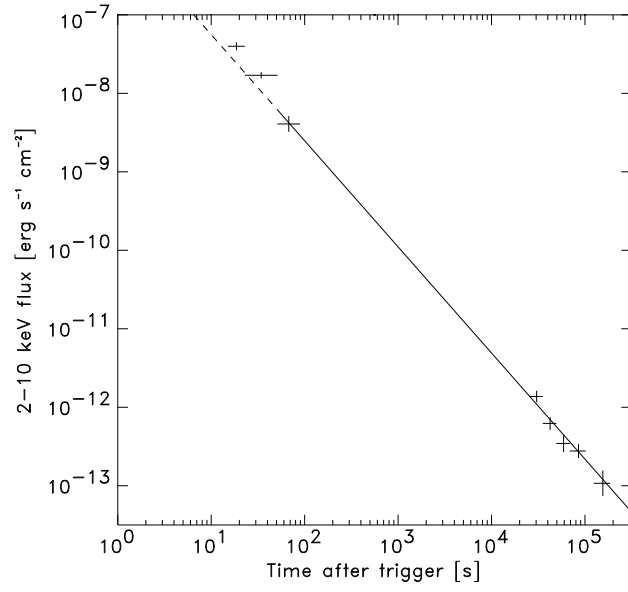


Fig. 3.—